

THE STRAIN-RATE DEPENDENCE OF MECHANICAL PROPERTIES OF RABBIT KNEE LIGAMENTS

Sota Yamamoto

Akinori Saito

Kei Nagasaka

Satoshi Sugimoto

Koji Mizuno

Eiichi Tanaka

Nagoya University

Japan

Masaki Kabayama

Matsushita Electric Works, Ltd.

Japan

Paper Number 115

ABSTRACT

This study is concerned with the mechanical properties of knee joint ligaments, which are frequently injured in car-to-pedestrian collisions. Because of the lack of knowledge of the dynamic properties of these ligaments, there are some difficulties in finite element simulations of a car-to-pedestrian accident. Thus, we conducted tensile tests on the rabbit medial collateral ligament (MCL) and anterior cruciate ligament (ACL) to evaluate the strain-rate dependence of their mechanical properties. The failure stress of the MCL increased with the strain rate. The avulsion load of the MCL tibial insertion was lower than the failure load of the MCL in all conditions tested. Three types of failure patterns were observed in the femur-ACL-tibia complex. The tangent modulus and the maximum stress of the ACL complex increased with the strain rate. The strain-rate dependence of the mechanical properties of knee ligaments was evaluated quantitatively. The results are expected to be useful for discussion of the injury criteria for the knee joint and its protection.

INTRODUCTION

Knee ligaments contribute to the stability of knee joint by controlling excessive motions. When the knee joints are injured in car-to-pedestrian collisions or sports accidents, the ligaments are frequently damaged because of the large external force exerted on the joints. Such injuries lead to many disabilities in actions in daily life and require a long time for healing and rehabilitation. Moreover, it is not easy to recover ligament the original functions when they have been ruptured. Thus, to clarify the mechanism of knee injury is important for pedestrian protection and better QOL from the viewpoints of orthopaedics and injury prevention engineering. Recently, dynamic finite

element analysis is coming into considerable use in studies of injury prevention, for example Takahashi et al.^[1] However, few data have been reported on the mechanical properties of knee joint ligaments at the high strain-rate found in car-to-pedestrian collisions. For example, Woo et al.^[2] performed tensile tests for rabbit medial collateral ligaments (MCL) and showed that the failure stress, strain and tangent modulus increased with strain-rate. Yamamoto et al.^[3] found that failure stress and strain increased with strain-rate but that the tangent modulus did not show rate dependence. As mentioned above, the strain-rate dependency of the mechanical properties of the ligament is not sufficiently understood. Therefore, the mechanical properties of medial collateral ligament (MCL) and anterior cruciate ligament (ACL), which are frequently injured, must be elucidated for more accurate simulations.

In light of this background, we evaluated the strain-rate dependence of the mechanical properties of knee joint ligaments in the rabbit. We conducted tensile tests on the rabbit MCL at various strain rates and discussed the strain-rate dependence of mechanical properties of the substance and tibial insertion of the MCL. We also performed tensile tests on the femur-ACL-tibia complex and evaluated its failure.

MATERIALS AND METHODS

Preparation of MCL

The mechanical properties of the MCL were evaluated in two regions: ligament substance and tibial insertion of the MCL. The mechanical properties of the ligament substance were evaluated by tensile tests using femur-MCL complex specimens. The strength of tibial insertion of the MCL was evaluated using MCL-tibia complex specimens.

Specimens of the ligament substance were obtained from 16 Japanese white rabbits (female, 2.8 ± 0.17 kg, mean \pm S.D.). The animals were sacrificed by injecting an overdose of pentobarbital sodium. The MCL was then removed together with the distal femur and proximal tibia. Next, the femur-MCL-tibia complex was attached on a laser width meter type cross-sectional area meter^[4], and its cross-sectional area was measured under 0.5 N loading. The tibial insertion of MCL was then detached to avoid avulsion. The distal end of the MCL was fixed on a metal jig with cyanoacrylate cement. The femur was embedded in resin to make the femur easy to fix for the tensile test. Two dot markers were added at a 5-mm interval on the surface of the

MCL substance using nygrosin to measure the MCL strain.

Specimens of the tibial insertion were obtained from 13 Japanese white rabbits (female, 3.0 ± 0.13 kg, mean \pm S.D.) and prepared by a procedure similar to that for the ligament substance specimens. The femoral insertion of the MCL was detached and the proximal end was fixed on a metal jig with cyanoacrylate cement. The tibia was embedded in resin. It is not easy to define the strain and cross-sectional area at the tibial insertion because the insertion is attached on the flat part of the medial side of the proximal tibia. Thus, the markers using nygrosin were omitted for the tibial insertion specimens.

During all preparation procedures described above, the MCL was kept in wet condition by appropriate drip-application of physiological saline solution.

Preparation for ACL

Seven Japanese white rabbits (female, 3.0 ± 0.17 kg, mean \pm S.D.) were used for ACL tests. Femur-ACL-tibia complex (FATC) specimens were used for the ACL tensile tests.

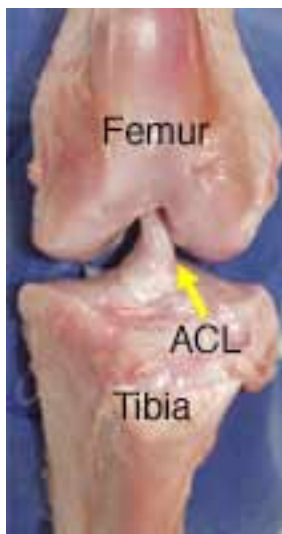


Figure 1. Frontal view of femur-ACL-tibia complex

First, a femur-knee joint-tibia complex was removed and then attached on a plastic jig to define the geometry of the knee joint in the maximum extended position. Because of the twisted and inclined ACL structure shown in Figure 1, attention must be paid to the geometry of the knee joint. Woo et al. reported that the loading direction influences the failure properties of ACL^[5], making the flexion angle of knee joint the most important geometrical parameter. Since our main focus is pedestrian protection, the human standing posture should be simulated in the experiments. To evaluate the

knee joint geometry of the rabbit corresponding to the human standing posture, the angle between the femur and tibia was examined in the maximally extended position as shown in Figure 2. The joint angle was defined as the angle between the line passing through the malleous lateralis and lateral condyle of the tibia and the line passing through the

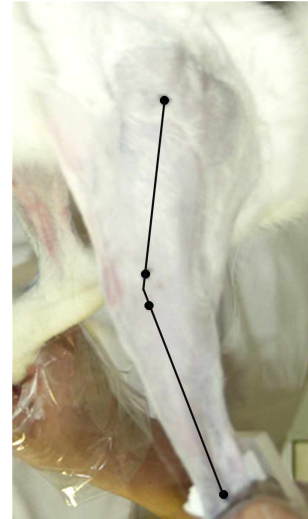


Figure 2. Maximum extended posture of rabbit knee joint

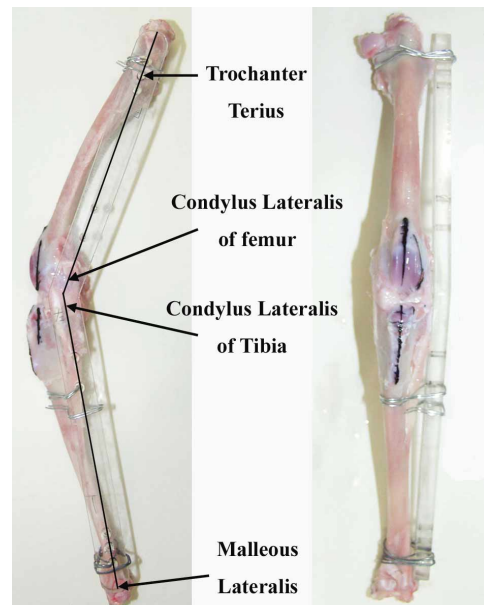


Figure 3. Femur-knee joint-tibia complex fixed on a jig at maximum extended knee angle

trochanter terius and lateral condyle of the femur. The maximum joint angle of a sacrificed rabbit was about 150° , so this value was used for the experimental set up

of the femur-ACL-tibia complex. The femur-knee joint-tibia complex was extended and fixed at a 150° joint angle on the jig. Two line marks were then put on the frontal and lateral surfaces of the femur and tibia using nygrosin (Figure 3).

These line markers were used as a reference to adjust the geometry of the knee joint when the specimen was chucked on the tensile test system. The surrounding soft tissue, the proximal femur and the distal tibia were then removed. The cross-sectional area of the ACL midsection was measured in a non-twisted position by the measuring system^[4] described above. The medial condyle and lateral condyle of femur were removed for the laser width meter measuring. A schematic drawing of the shape of the distal femur is shown in Figure 4.

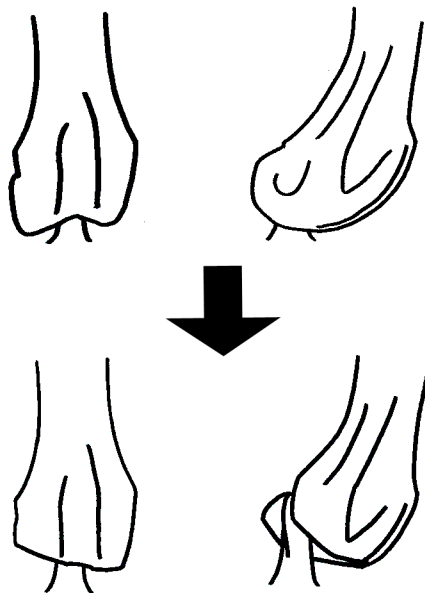


Figure 4. Schematic drawing of shaped femur condyle of specimen

The length of the ACL and width of its tibial insertion were also measured at the maximum joint angle by a vernier caliper. The definitions of these morphological parameters were shown in Figure 5. Then the distal femur and proximal tibia were embedded in resin. Finally, two dot markers were added on the frontal edges of the femoral and tibial condyle using nygrosin to measure the strain of the ACL. The ACL was kept in a wet condition by appropriate drip-application of physiological saline solution.

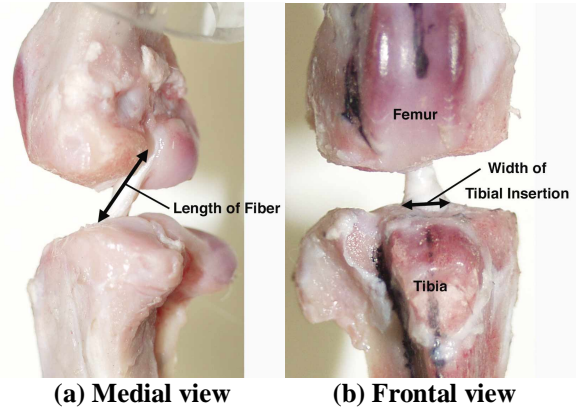


Figure 5. Definition of ACL morphological parameters

Set up for MCL tensile tests

A previously-developed dynamic/quasi-static tensile test system^[4] was used. A schematic diagram of the system equipped with an AC servomotor and an N₂ gas actuator is shown in Figure 6. The velocity ranges of the servomotor and gas actuator are sequential, i.e., the servomotor works as the actuator for quasi-static tests when the elongation rate is between 0.01 mm/sec and 10 mm/sec, and the N₂ gas actuator is used for dynamic tests when the elongation rate is over 100 mm/sec. The force applied to a specimen was measured by a load cell on the piston.

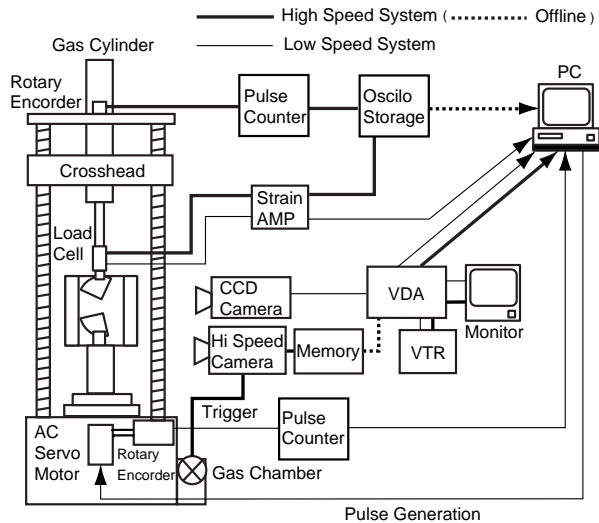


Figure 6. Schematic diagram of tensile test system for MCL substance and tibial insertion.

The signals of the load cell and rotary encoder mounted on the piston are stored on a digital oscilloscope (Sony Techtronix, TDS420A). The relative displacement

between the markers on the MCL was recorded by a high-speed video camera (Kodak, HS-4540) for the dynamic test or a CCD camera (Hamamatsu Photonics, C5405) for the quasi-static test. The strain of the MCL substance was measured by a VDA (Hamamatsu Photonics, C3162). Both femur-MCL and MCL-tibia complexes were fixed on the test system in the position in which the longitudinal direction of MCL was aligned with the loading direction. The extension-rate conditions were set as 0.01, 0.3 and 10 mm/sec for quasi-static tests and 100 and 300 mm/sec for dynamic tests. All experiments were performed in 37°C physiological saline solution.

Set up for ACL tensile test

The same tensile test system used for the MCL experiments was employed for the ACL tensile test. Only the strain measuring method was changed. The relative displacement of the markers was recorded using a digital video camera recorder (DCR-VX2000, SONY) in quasi-static conditions and a digital high-speed video camera (MEMRECAM fx-K3, NAC Image Technology) in dynamic conditions, and analyzed using a video analyzing software (Movious Pro, MIRA). All of the tests were performed in 37°C physiological saline solution.

The specimen was chucked with reference to the line markers on the frontal and medial surface of the femur-ACL-tibia complex with 0.5 N preloading. The loading direction was defined as shown in Figure 7, and the extension rate was set at 0.01 mm/sec and 200 mm/sec.

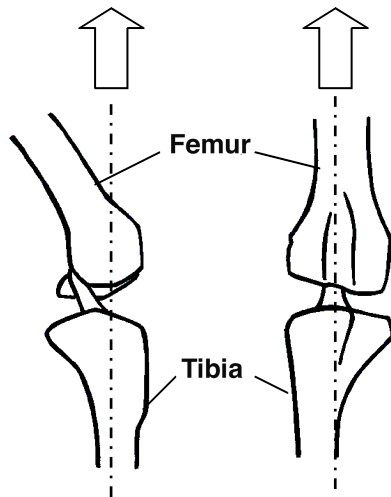


Figure 7. Definition of loading direction for femur-ACL-tibia complex

RESULTS AND DISCUSSION

Mechanical properties of MCL substance

The measured strain rate for each extension-rate condition is shown in Table 1. The extension rate was estimated as the cross-head velocity for quasi-static tests and the piston velocity for dynamic tests. The strain rate was calculated as the relative velocity between the two nygrosin markers.

The stress-strain curves of the MCL substance with various strain-rate conditions are shown in Figure 8. For the curves with 0.055 and 1.2%/sec strain rate, we could see typical toe regions in low strain range and convex shape in the strain range over 5%, however linear relations were observed in the stress-strain curves with 27.4, 653 and 1007%/sec strain rate.

Table 1.
Extension-rate conditions and corresponding strain-rate conditions for ligament substance of MCL

Extension Rate (mm / sec)	Strain Rate (% / sec)
0.01	0.055 ± 0.019
0.3	1.202 ± 0.106
10	27.4 ± 5.76
95.6 ± 9.6	653 ± 118
278 ± 27	1007 ± 256

(Mean ± S.D.)

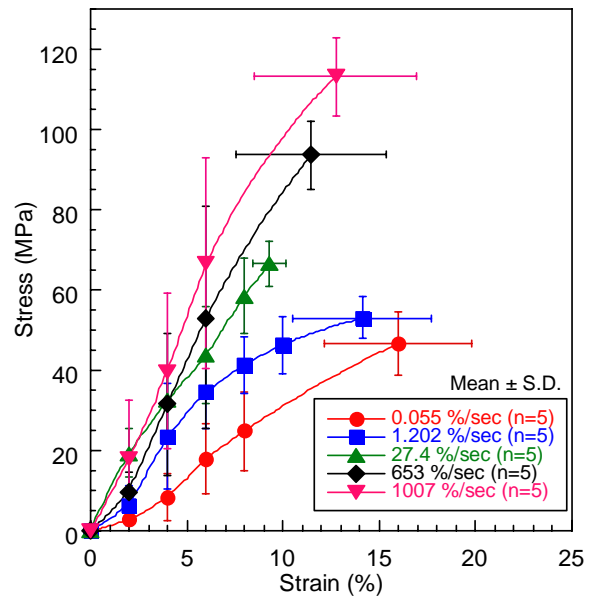


Figure 8. Stress-strain relation of MCL ligament substance

The tangent moduli were evaluated in Figure 9 and defined as the moduli in the section between 3 to 7% for quasi-static tests and in the section between 2 to 6% for dynamic tests. The result of statistical analysis with one-way ANOVA did not show a significant difference among tangent moduli in each strain-rate condition ($p > 0.05$). On the other hand, the failure stress increased with the strain rate and showed a statistically significant difference ($p < 0.05$, one-way ANOVA). This correlation is the same as that of the maximum stress of the femur-MCL-tibia complex^[4].

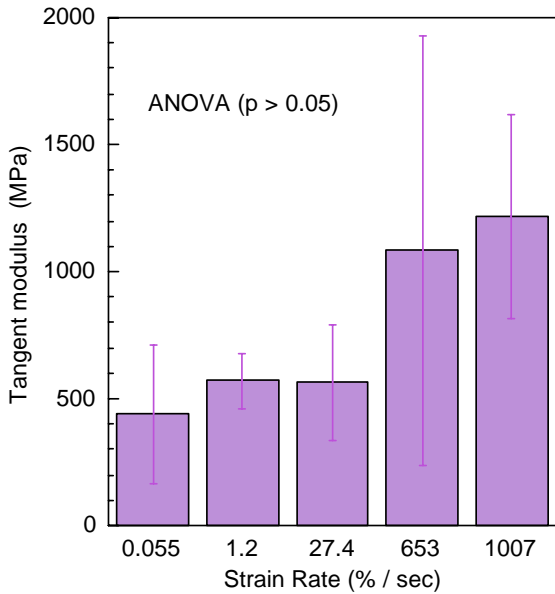


Figure 9. Tangent moduli of stress-strain curve of MCL ligament substance

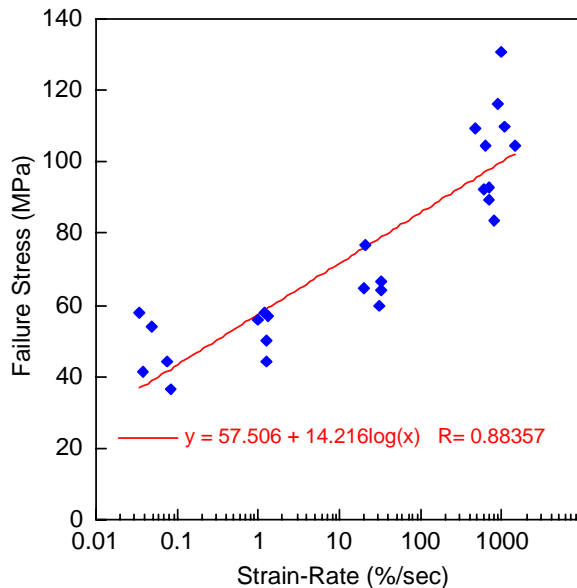


Figure 10. Strain-rate dependence of failure stress of MCL ligament substance

Figure 10 shows the correlation between strain rate and failure stress in MCL substance. We obtained a logarithmic regression function with a high multiple correlation coefficient. This function shows the strain-rate dependence of the failure stress of the MCL substance. In contrast, the failure strain did not show a significant difference among each of the strain-rate conditions ($p > 0.05$).

Strength of tibial insertion of MCL

The failure loads of tibial insertion in each extension-rate condition are shown in Figure 11, which also shows the failure loads of the MCL substance at various extension-rates. The failure load of the tibial insertion increased with the strain rate, and a statistically significant difference was observed with each experimental condition ($p < 0.05$). Thus, the strength of tibial insertion appears to depend on the strain rate just as with the failure stress of the MCL substance. The failure load of the tibial insertion is smaller than that of the MCL substance in all extension-rate conditions. This suggests that the tibial insertion is the most dangerous site in the femur-MCL-tibia region. However, an MCL rupture was observed at a high strain-rate condition in our former study in which femur-MCL-tibia complex used for a specimen^[4]. In the present study, we removed the femoral insertion of the MCL in the preparation. That manipulation can cause loosening and inhomogenous tension of the collagen in the MCL, leading to possible

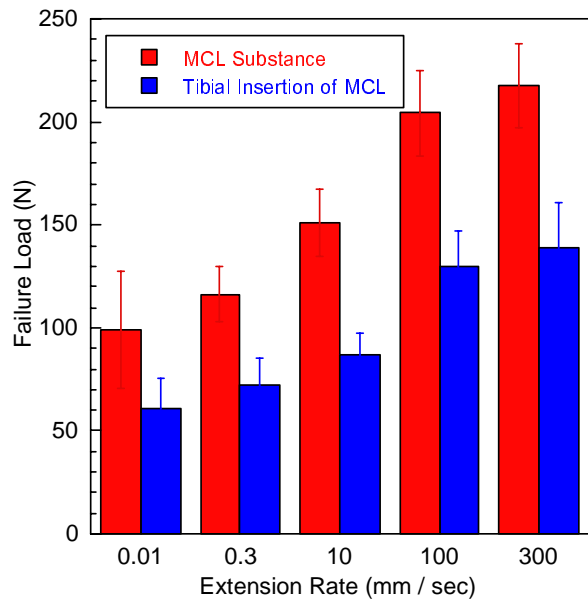


Figure 11. Comparison between failure load of MCL tibial insertion and ligament substance at various strain rates

underestimation of the failure load of the tibial insertion. In the experiments with the MCL substance, no fracture and avulsion were found in the femoral insertion of the MCL. The collagenous tissue of the MCL inserts into the medial condyle of femur and is tightly connected. On the other hand, the tibial end of the MCL is attached on the periosteum of the medial side of the proximal tibia. Such a structural characteristic causes a difference in the strength between the femoral insertion and the tibial insertion of the MCL. In the results of the cadaver test in which a car-to-pedestrian accident was simulated, an avulsion fracture of the femoral insertion of MCL was observed^{[6] [7]}. This type of injury was not observed in the current study. Thus, it is considered that such an avulsion fracture of the femoral insertion can be simulated by a lateral loading experiment. Experiments in which the loading condition in a real accident is considered are therefore needed.

Failure properties of femur-ACL-tibia complex

The measured strain rate for each extension-rate condition is shown in Table 2. Three types of failure patterns were observed: avulsion fracture at femoral insertion, avulsion fracture at tibial insertion and epiphysiolysis of femoral distal condyle. These three failure patterns can be seen in traffic or sports accidents. Photos of typical failure patterns are shown in Figure 12.

Table 2.

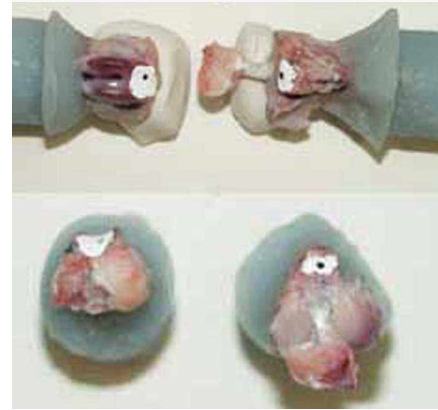
Extension-rate conditions and corresponding strain-rate conditions for femur-ACL-tibia complex

Extension Rate (mm / sec)	Strain Rate (% / sec)
0.009	0.155 ± 0.020
173.6 ± 13.4	2249 ± 294

(Mean ± S.D.)

The ratios of the frequency of each ACL failure pattern are shown in Figure 13. In quasi-static tests, epiphysiolysis was the major failure pattern. On the other hand, the frequencies of every failure pattern were equal in the dynamic test condition.

Figure 14 shows load-elongation curves of the femur-ACL-tibia complex in each test condition. With both extension rates, the load-elongation curves showed the nonlinear relation typically seen for biological soft tissue. The failure load tends to increase with the extension rate.



(a) Avulsion fracture at femoral insertion of ACL



(b) Avulsion fracture at tibial insertion of ACL



(c) Epiphysiolysis of femoral distal condyle

Figure 12. Photos of typical failure patterns of femur-ACL-tibia complex

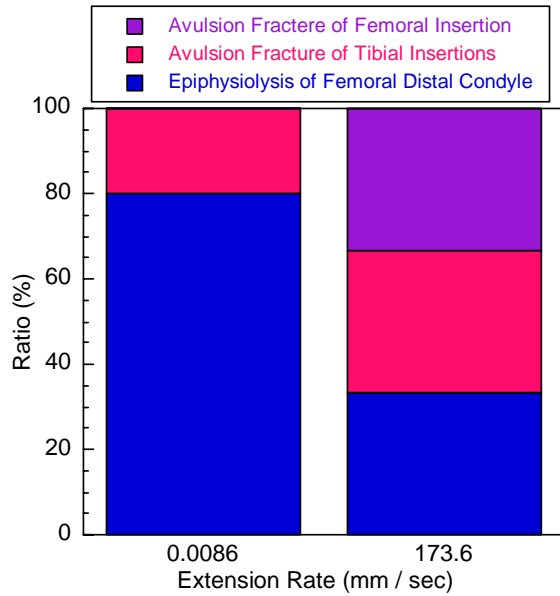


Figure 13. Distributions of failure patterns of femur-ACL-tibia complex

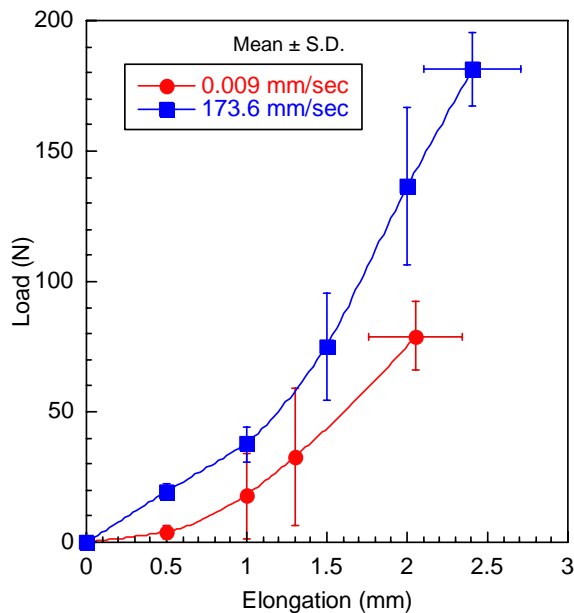


Figure 14. Load-elongation curves of femur-ACL-tibia complex at various extension rates

The stress-strain relation was evaluated based on the load-elongation relation and the cross-sectional area at the ACL midsubstance as shown in Figure 15. It must be noted that these stress-strain relations do not indicate the exact mechanical properties of the ACL because the loading direction is not parallel to the longitudinal axis of the ACL. This figure indicates an apparent stress-strain relationship. To discuss the strain-rate

dependence of stress-strain relation, the tangent modulus was calculated in the 20 - 25% strain range for dynamic tests and in the 6 - 10 MPa stress range for quasi-static tests. The tangent modulus for each condition was shown in Figure 16. The tangent modulus showed a statistically significant difference in strain rate ($P < 0.05$, Student's t test). The tangent

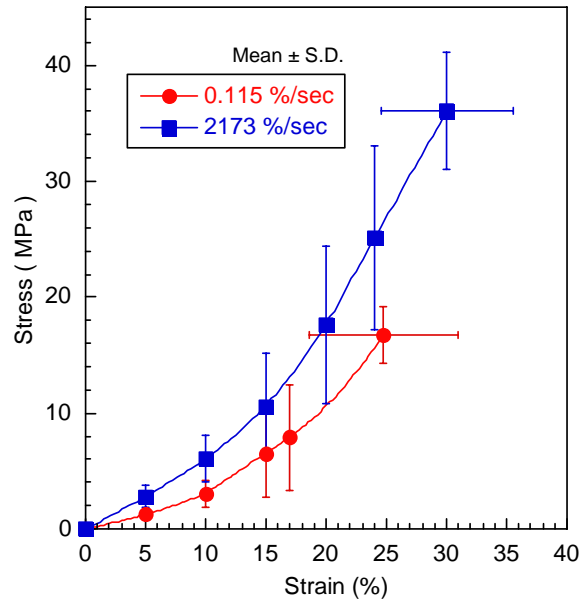


Figure 15. Stress-strain curves of femur-ACL-tibia complex at various strain rates

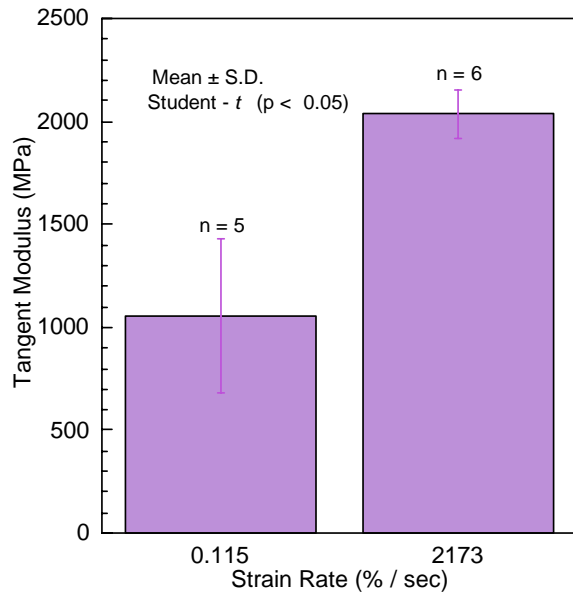


Figure 16. Tangent moduli of stress-strain curve of femur-ACL-tibia complex at various strain rates

modulus of the ACL was about twice of that of the MCL. Woo et al.^[8] showed the tangent modulus of ACL is half as that of MCL in a quasi-condition. To discuss these two different results the actual stress-strain relation of ACL must be evaluated. The maximum stress and strain were also analyzed statistically. As shown in Figure 17 and 18, the maximum stress significantly increased with the strain

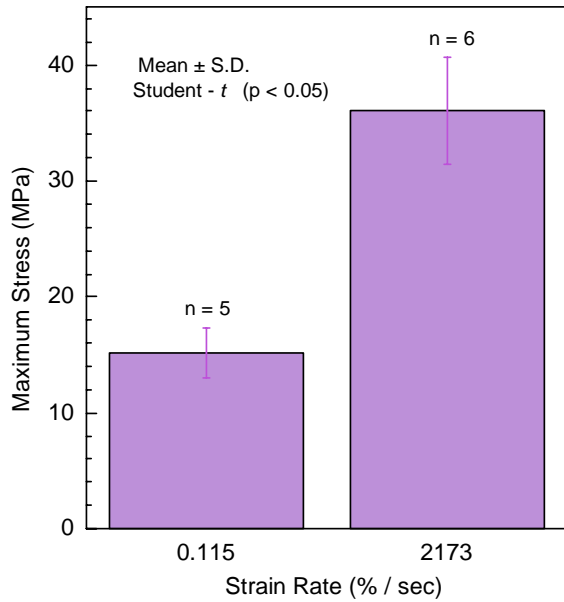


Figure 17. Maximum stress of femur-ACL-tibia complex at various strain rates

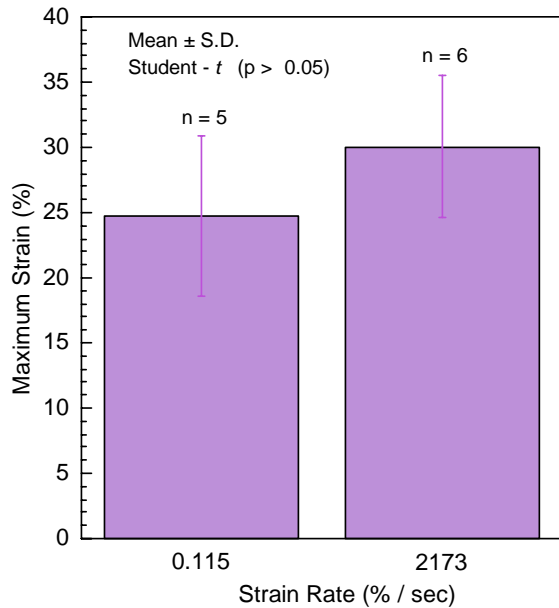


Figure 18. Maximum strain of femur-ACL-tibia complex at various strain rates

rate ($P < 0.05$, Student's t test) but the maximum strain did not depend on the strain rate ($P > 0.05$, Student's t test).

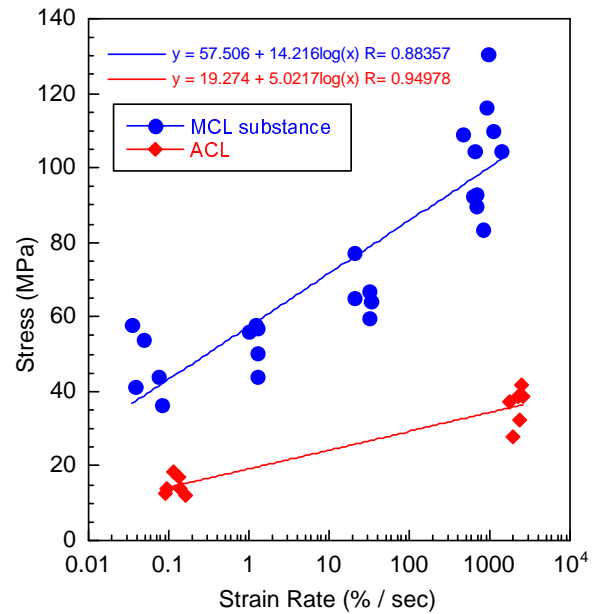


Figure 19. Strain-rate dependence of failure stress of femur-ACL-tibia complex and MCL ligament substance

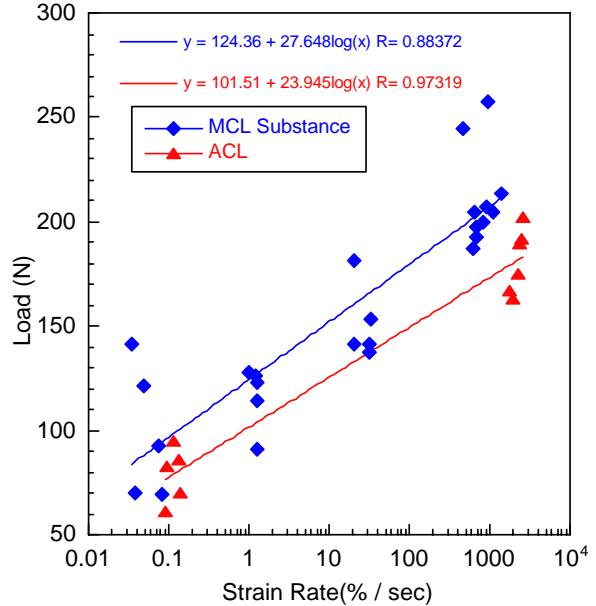


Figure 20. Strain-rate dependence of failure load of femur-ACL-tibia complex and MCL ligament substance

Figure 19 shows the correlation between the strain rate and maximum stress of the femur-ACL-tibia complex. It also contains the data on the MCL substance. In a

comparison between the rate-dependence of the ACL and MCL, the coefficient of logarithmic regression function for the ACL was smaller than that of MCL. But when we compare the maximum load of the femur-ACL-tibia complex and the failure load of the MCL substance, the difference in the coefficient of regression functions decreases (Figure 20).

The strain-rate dependence of the failure properties of the femur-ACL-tibia complex looks similar to those of the MCL substance. However, the maximum stress and strain discussed here may underestimate the failure properties of ACL because epiphysiolysis of the femoral distal condyle occurred with high frequency in this study. The cause of this high frequency could be the immaturity of the experimental animals. This disturbance may disappear with a more suitable experimental set up.

No rupture in the ACL was observed in the tensile tests, unlike the case for traffic accidents. In a real-world accident, while axial tensile load is rarely applied, the shearing or bending load is likely to be applied. Therefore, other types of loading test, for example medial-lateral shearing or anterior drawer test, must be performed.

CONCLUSIONS

Mechanical properties of knee ligaments were discussed in the present study as a means to contribute to pedestrian protection. The strain-rate dependence of these properties was evaluated by quasi-static and dynamic tensile tests on the rabbit knee joint, and the following results were obtained.

- (1) The failure stress of the MCL ligament substance significantly increased with the strain rate, but the failure strain and the tangent modulus did not depend on the strain rate.
- (2) The failure load of the tibial insertion of the MCL is lower than that of the MCL ligament substance.
- (3) Three types of failure, avulsion fracture at the femoral and tibial insertion of the ACL and the epiphysiolysis of femoral distal condyle, were observed in the tensile tests on the femur-ACL-tibia complex.
- (4) The tangent modulus and maximum stress of the femur-ACL-tibia complex showed a significant strain-rate dependence.
- (5) No rupture in the ACL substance was observed. To simulate the actual loading conditions in real-world accidents, other types of loading test, for example a

medial-lateral shearing or anterior drawer test, should be performed as the next step.

REFERENCES

- [1] Takahashi, Y., Kikuchi, Y. et al. 2000. "Development and Validation of the Finite Element Model for the Human Lower Limb of Pedestrians." STAPP Car Crash Journal Vol. 44 Paper No. 2000-01-SC22.
- [2] Woo SL-Y, Peterson RH et al. 1990. "The Effects of Strain Rate on the Properties of the Medial Collateral Ligament in Skeletally Immature and Mature Rabbits: A Biomechanical and Histological Study." J Orthopaedic Res: 8, No.5, 712-721.
- [3] Yamamoto N, Hayashi K. 1998. "Mechanical Properties of Rabbit Patellar Tendon at High Strain Rate." Bio-Medical Materials and Engin: 8, 83-93.
- [4] Yamamoto S, Kajzer J et al. 2000. "Development of High-Speed Tensile Test System for Ligaments and Skeletal Muscles." Human Biomechanics and Injury Prevention, ed. by Kajzer J, Tanaka E, Yamada H, Springer Verlag Tokyo, 167-172.
- [5] Woo, S.L-Y. et al. 1987. "Effects of Knee Flexion on The Structural Properties of The Rabbit Femur-Anterior Cruciate Ligament-Tibia Complex (FATC)." Journal of Biomechanics Vol. 20, No.6, pp. 557-563.
- [6] Kajzer J., Schroeder G. et al. 1997. "Shearing and Bending Effects at the Knee Joint at High Speed Lateral Loading." SAE Paper No.973326, 41st STAPP.
- [7] Kajzer J., Schroeder G. et al. 1999. "Shearing and Bending Effects at the Knee Joint at Low Speed Lateral Loading." SAE Paper No. 1999-01-0712, Occupant Protection SAE SP-1432.
- [8] Woo, S.L-Y., Newton, O., et al. 1992. "A Comparative Evaluation of The Mechanical Properties of The Rabbit Medial Collateral and Anterior Cruciate Ligaments." Journal of Biomechanics Vol. 25, No.4, pp. 337-386.